

# Earth-skimming UHE Tau Neutrinos at the Fluorescence Detector of Pierre Auger Observatory

C. Aramo<sup>1</sup>, A. Insolia<sup>2</sup>, A. Leonardi<sup>2</sup>, G. Miele<sup>1</sup>, L. Perrone<sup>3</sup>, O. Pisanti<sup>2</sup>,  
D.V. Semikoz<sup>4,5</sup>

<sup>1</sup> *Dipartimento di Scienze Fisiche, Università di Napoli “Federico II” and Istituto Nazionale di Fisica Nucleare Sezione di Napoli, Complesso Universitario di Monte S. Angelo, Via Cinthia, I-80126 Napoli, Italy.*

<sup>2</sup> *Dipartimento di Fisica e Astronomia, Università di Catania and Istituto Nazionale di Fisica Nucleare Sezione di Catania, Via S. Sofia 64, I-95123 Catania, Italy.*

<sup>3</sup> *Fachbereich C, Sektion Physik, Universität Wuppertal, D-42097 Wuppertal, Germany.*

<sup>4</sup> *Department of Physics and Astronomy, UCLA, Los Angeles, CA 90095-1547 USA.*

<sup>5</sup> *INR RAS, 60th October Anniversary prospect 7a, 117312 Moscow, Russia.*

## Abstract

Ultra high energy neutrino fluxes produced either by the interaction of hadronic cosmic rays with the cosmic electromagnetic radiation background or by new exotic hadrons or topological defects might be detected in the new generation of giant experimental apparatus as the Pierre Auger Observatory. The viable detection strategy, which applies to tau neutrinos only, concerns the almost horizontal Earth-skimming events which can be detected by the Fluorescence Detector. A detailed analysis of such a possibility is here carried out for a quite wide class of neutrino flux models. In order to get a more reliable prediction for the number of events, an updated computation of the neutrino–nucleon cross section and of the corresponding average inelasticity parameter is here performed. For the most optimistic theoretical models Auger FD will see order one Earth–skimming neutrino event in several years of observation.

*PACS numbers: 95.85.Ry, 13.15.+g, 96.40.Tv, 95.55.Vj, 13.35.Dx;*

# 1 Introduction

The new generation of giant cosmic rays apparatus on the Earth surface, like the Pierre Auger Observatory (PAO) [1], under ice or water, like AMANDA/Icecube, Baikal, RICE, ANTARES, NESTOR [2]-[7], from balloon, like ANITA [8], or in space, like EUSO [9], are just to unveil the features of the most violent astrophysical phenomena, where hadronic matter is accelerated almost up to the speed of light. By detecting UHE  $\nu$ 's these new apparatus will be able to trace back their possible astrophysical sources, and thus will represent the beginning of neutrino astronomy.

The existence of a sensible neutrino flux with energy above  $10^{17}$  eV is expected from the interaction of UHE cosmic rays, which have been detected by several experiments, i.e. Volcano Ranch [10], Haverah Park [11], Fly's Eye [12], Yakutsk [13], AGASA [14] and HiRes [15], with the Cosmic Microwave Background (CMB) *via* the  $\pi$ -photoproduction,  $p + \gamma_{CMB} \rightarrow n + \pi^+$ , the so-called *cosmogenic neutrinos* [16]. The prediction for such a flux is however affected by several uncertain physical quantities, namely the spatial distribution of astrophysical sources, the ejected proton fluxes (if proton) and the way of modelling the diffuse extragalactic electromagnetic background in the different frequency regions. One can assume reasonable ansatz for all this quantities and then use the information about the diffuse photon flux in the GeV region, measured by the EGRET detector on board of the Compton- $\gamma$  ray observatory [17], and the AGASA/Hires measurements of UHE cosmic rays to constrain the value of the model free parameters. An exhaustive analysis of these models and the prediction of more exotic scenarios have been presented in a series of papers (see for example Ref.s [18, 19]).

Such energetic neutrinos, once produced, are hardly detected, as they are almost completely shadowed by Earth and rarely interact with the atmosphere. An EeV neutrino has in fact an interaction length of the order of 500 Km water equivalent in rock and, even crossing horizontally the atmosphere, the 360 meters water equivalent will stop only one neutrino among about one thousand passing through. Due to either the very low expected flux for such energetic particles, namely less than 1 particle/year/km<sup>2</sup>, or the small neutrino-nucleon cross section, both km<sup>3</sup>-neutrino telescopes and giant surface

detectors looking at atmospheric events have very few chances to catch such energetic particles.

In this framework, the most interesting detection strategy proposed concerns  $\nu_\tau$  only [20]-[28], and is related to the very different behaviour in crossing matter of tau-lepton with respect to muons or electrons. As shown for example in Figure 1 of Ref. [25], for energy values between  $10^{18}$  and  $10^{21}$  eV the  $\tau$  decay length is not much larger than the corresponding interaction range. Thus such an energetic  $\tau$ , if produced not too deep under the surface of the Earth by the corresponding neutrino, has a finite probability to emerge in the atmosphere as an upgoing particle. This is completely different from the muon case where the charged lepton crossing through the rock rapidly loses energy and decays, being so stopped in the rock. Almost horizontal  $\nu_\tau$ , just skimming the Earth surface, will cross an amount of rock of the order of their interaction length and thus will be able to produce a corresponding  $\tau$ , which in principle might shower in the atmosphere and be detected. In order to estimate the number of upgoing  $\tau$  expected in an experimental set up as for example the Pierre Auger Observatory one needs to know, with a reasonable confidence level, the value of the neutrino-nucleon cross section for the Charged Current (CC) Interaction,  $\nu_\tau + N \rightarrow \tau + X$ , and the inelasticity parameter,  $y = 1 - E_\tau/E_\nu$ , in the relevant region of four momentum transferred,  $Q^2$ , and Bjorken  $x = Q^2/(2 M y E_\nu)$ .

The aim of this paper is to estimate the number of possible upgoing  $\tau$  showers which the Fluorescence Detector (FD) of PAO could detect. The predictions are analyzed with respect to their dependence on the cosmogenic neutrino fluxes and by using a new estimate for both  $\nu - N$  cross section and the inelasticity parameter. The paper is organized as follows. Section 2 is devoted to a brief but exhaustive discussion of the different models for neutrino flux predictions. In section 3, the general features of deep inelastic neutrino cross sections are outlined for neutrino energies up to  $10^{21}$  eV. In section 4, high energy  $\tau$  propagation through matter is illustrated by considering all the relevant interaction mechanisms. Average values for  $\tau$  energy loss are provided by taking into account the recent calculations of photonuclear interaction given in Ref. [30]. In section 5 the expression for the number of upgoing  $\tau$  showers is obtained and discussed. Finally in section 6 we give our conclusions and remarks.

## 2 Neutrino flux estimates

Highest energy protons with energy above  $E_{th} \approx 10^{20}$  eV travelling in the cosmo will lose their energy in interactions with CMB radiation and other photon backgrounds and produce pions. Charged pions,  $\pi^\pm$ , will eventually decay in charged leptons and neutrinos, while neutral pions,  $\pi^0$ , will produce high energy gamma rays. Neutrinos produced in interactions of UHECR protons with CMB are called cosmogenic neutrinos [16].

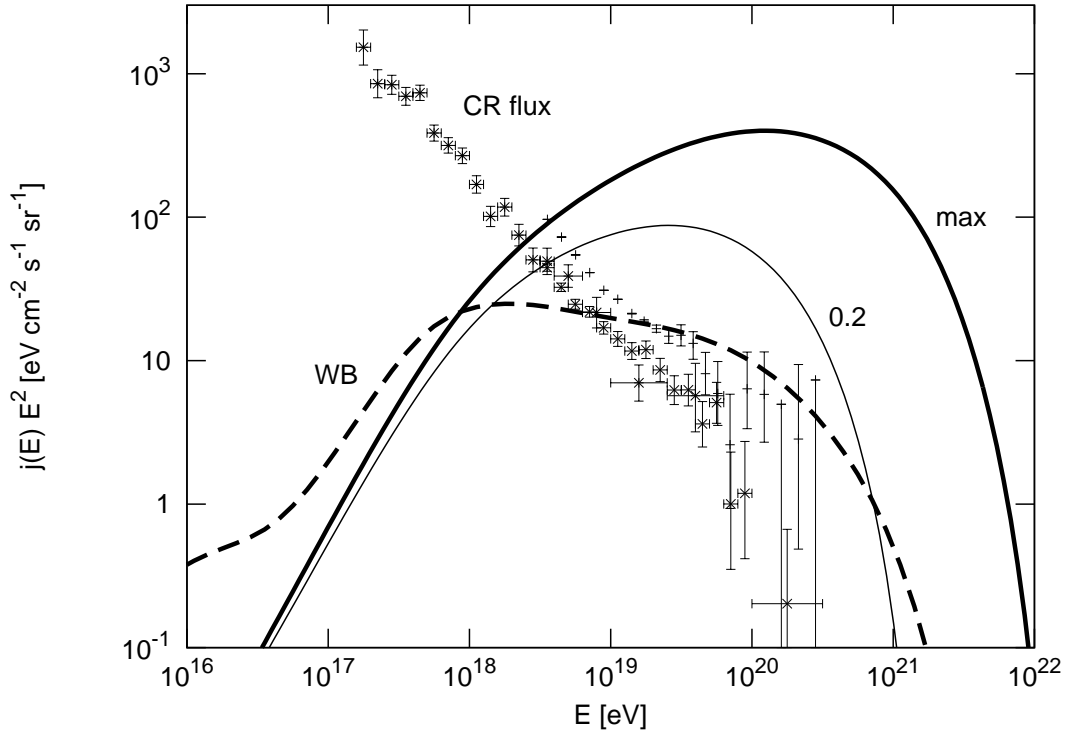


Figure 1: Flux of cosmogenic neutrinos as a function of the energy. Solid line represents the flux upper bound, thin solid line is for 1/5 contribution in the EGRET flux (see text) and dashed line is for the case of  $1/E^2$  initial proton flux, or so called Waxman-Bahcall limit. The points represent the UHECR flux measured by AGASA and HiRes.

All secondary gamma rays and electrons will lose their energy in electromagnetic cascade which will end up at GeV level. At this energies extragalactic diffuse gamma-ray background was measured by the EGRET experiment [31]. This measurement provides the upper bound on possible neutrino flux produced through pion production in any model. In particular it will give upper bound on the maximal possible flux of cosmogenic neutrinos or neutrinos from UHECR protons [32]. It is worth noticing that, since at

least part of UHECR are protons, the existence of cosmogenic neutrinos is guaranteed. However, the flux of cosmogenic neutrinos is very uncertain. In Figure 1 we plot the GZK neutrino flux for three possible scenarios. Thick solid line represents the case of an initial proton flux  $\propto 1/E$  and maximum contribution of produced photons in the EGRET region (GZK-H). Thin solid line shows the neutrino flux when the associated photons contribute only up to 20 % in the EGRET flux (GZK-L). Dashed line stands for the conservative scenario of an initial proton flux  $\propto 1/E^2$  (GZK-WB); in this case the neutrino flux is compatible with the so-called Waxman-Bahcall limit [33]. Note that cosmogenic neutrino flux has no lower bound. In particular, in the most conservative, but rather unrealistic, case astrophysical sources cannot accelerate protons up to energies above GZK cutoff and thus the secondary neutrinos will be produced in negligible quantities. All neutrino fluxes presented in this section were calculated by means of a propagation code [34] which takes into account production of neutrinos in proton interactions with CMB, infrared/optical and radio photon backgrounds as well as neutron decay.

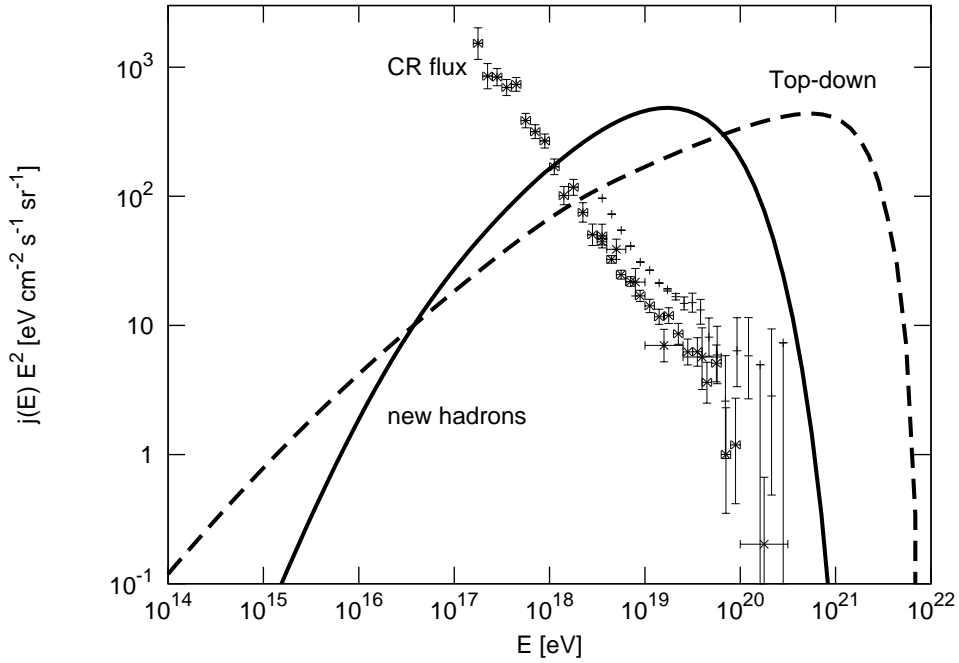


Figure 2: Neutrino fluxes in exotic UHECR models. Solid line is the neutrino flux in model of new hadrons whereas dashed line is the neutrino flux in topological defect model.

In most of the models which try to explain highest energy cosmic rays ( $E > 10^{20}$  eV)

in terms of exotic particles, an associated large flux of neutrinos connected to their decay or production is predicted. In Figure 2 we plot the expected neutrino flux for two of such models. One of them is the model of new hadrons [35] (NH). In this scenario UHECR events above GZK cutoff are due to new hadrons with mass  $M \sim 2-5$  GeV. For example, in SUSY models such particles can be bound states of light bottom squarks or gluinos. New hadrons can be produced in the astrophysical objects and reach Earth without significant energy losses in interactions with CMB radiation. However, the production of new hadrons is a subdominant process and it is accompanied by a large flux of neutrinos, shown in Figure 2 by a solid line, and gamma-rays from pion decays.

The dashed line in Figure 2 shows the neutrino flux for a Topological Defects model (TD) (for review see [36]). In this case UHECR events with energy  $E > 10^{20}$  eV are explained in terms of  $\gamma$ 's which are produced in the decay of heavy particles with mass of the order of  $10^{22-23}$  eV. Again, neutrino fluxes for this kind of models are unavoidably large.

We do not discuss here the so-called Z-burst scenarios, which attempts to explain UHECR as products of Z-boson decay, because they are strongly disfavored [19] by the upper bounds on UHE neutrino flux put by FORTE [37] and GLUE [38] experiments combined with the cosmological limits on neutrino mass by WMAP and LSS data [39].

In the following sections we will estimate the sensitivity of PAO to the UHE tau neutrino flux both in the case of cosmogenic neutrinos (Figure 1) and in the case of exotic models (Figure 2).

### **3 Neutrino-Nucleon cross section in the extremely high energy limit**

At energy above 1 GeV neutrino-atoms interaction is dominated by the process of *Deep Inelastic Scattering* (DIS) on nucleons, since the contributions of both elastic and quasi-elastic interactions become negligible. The effect of the scattering with atomic electrons will not be taken into account here, since the cross section for this process is, at each

energy, about three order of magnitude lower than the neutrino-nucleon cross section<sup>1</sup>.

Detectable leptons are produced through CC interaction,

$$\nu_l(\bar{\nu}_l) + N \rightarrow l^-(l^+) + X \quad , \quad (3.1)$$

whereas Neutral Current (NC) interaction causes a modulation in the spectrum of the interacting neutrinos,

$$\nu_l(\bar{\nu}_l) + N \rightarrow \nu_l(\bar{\nu}_l) + X' \quad . \quad (3.2)$$

Total cross sections can be written in terms of differential cross sections as follows:

$$\sigma_{CC}^{\nu N}(E_\nu) = \int_0^{1-\frac{m_l}{E_\nu}} \frac{d\sigma_{CC}^{\nu N}}{dy}(E_\nu, y) dy \quad , \quad (3.3)$$

$$\sigma_{NC}^{\nu N}(E_\nu) = \int_0^1 \frac{d\sigma_{NC}^{\nu N}}{dy}(E_\nu, y) dy \quad , \quad (3.4)$$

where  $E_\nu$  is the energy of the incoming neutrino,  $m_l$  is the mass of the outgoing charged lepton and  $y$  is the inelasticity parameter, defined as:

$$y_{CC,NC} = 1 - E_l/E_\nu \quad , \quad (3.5)$$

and  $E_l$  is the energy of the outgoing charged (for CC) or neutral (for NC) lepton.

### 3.1 Deep inelastic neutrino cross sections

Energy (GeV)	$\langle y_{CC} \rangle$	$\langle y_{NC} \rangle$
$10^7$	0.2388	0.2449
$10^8$	0.2180	0.2223
$10^9$	0.2019	0.2052
$10^{10}$	0.1900	0.1928
$10^{11}$	0.1785	0.1821
$10^{12}$	0.1542	0.1601

Table 1: Average inelasticity parameter for CC ( $\langle y_{CC} \rangle$ ) and NC ( $\langle y_{NC} \rangle$ ) interaction at different incoming neutrino energy.

Tau neutrino-nucleon cross sections have been calculated following the approach of Ref. [40], based on the renormalization-group-improved parton model, and the most recent data for the quark structure functions of nucleons.

<sup>1</sup>The only exception is the resonant  $\bar{\nu}_e \rightarrow W^-$  production, occurring at  $E_{\bar{\nu}_e} = 6.3$  PeV, whose contribution to the total event rate remains nevertheless negligible [40].

Cross sections are written in terms of the Bjorken scaling variables  $y$  and  $x = Q^2/2ME_\nu y$ , where  $-Q^2$  is the invariant momentum transferred between the incoming neutrino and the outgoing lepton. Details of nucleon structure become important at very high-energy, where actually available data are very poor or totally missing. As a consequence, lack of knowledge of quark structure at very low  $x$  ( $x \ll 10^{-5}$ ) dominates the uncertainty of cross section calculations at very high-energy. We used the CTEQ6 [29] parton density functions in the DIS factorization scheme. The  $Q^2$ -evolution is realized by the next-to-leading order Dokshitzer-Gribov-Lipatov-Altarelli-Parisi equations Ref.s [41]–[44]. The CTEQ6 distributions are particularly suitable for high energy calculations since the numerical evolution is provided for  $((1.3)^2 < Q^2 < 10^8)$  GeV<sup>2</sup> and for  $x$  down to  $10^{-6}$  ( $E_\nu \sim 10^7$  GeV). Values outside this range are returned using extrapolation.

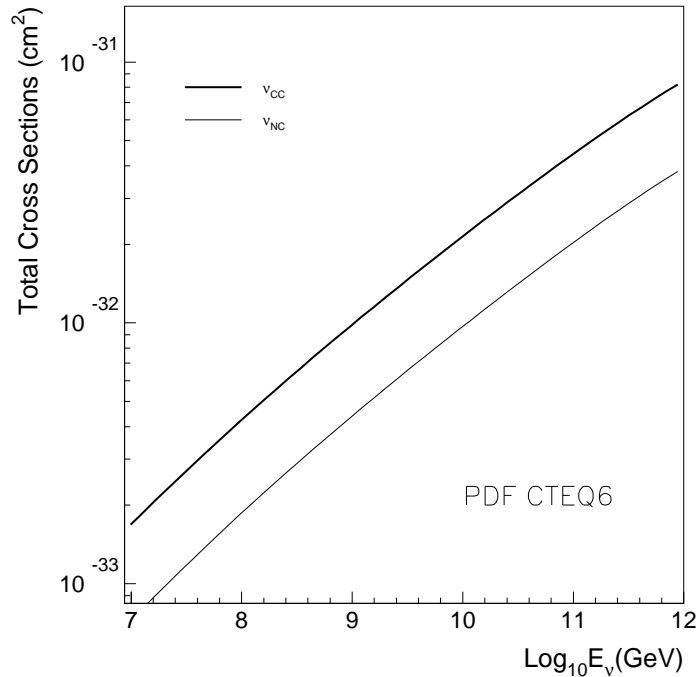


Figure 3: Total cross sections for CC (thick line) and NC (thin line) inelastic scattering off an isoscalar nucleon  $N = (n + p)/2$  by  $\nu_\tau$ . The calculation has been done for the CTEQ6 set of parton density functions [29], according to the prescription given in Ref. [40].

Total cross sections for  $\nu_\tau$  CC and NC inelastic scattering off an isoscalar nucleon,  $N = (n + p)/2$  ( $n = \#$  of neutrons,  $p = \#$  of protons), are shown in Figure 3. The



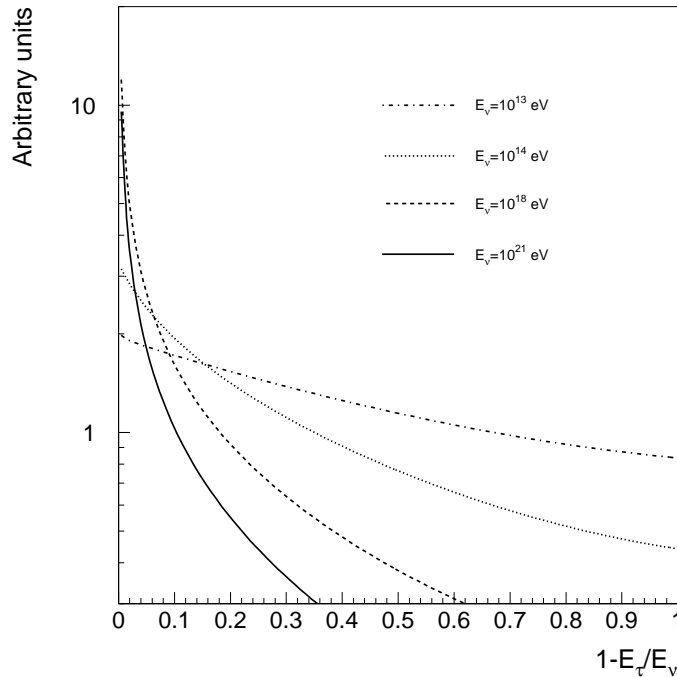


Figure 4: Distribution of the inelasticity parameter,  $y_{CC} = 1 - E_{\tau}/E_{\nu}$ , for different neutrino energies.

calculation for  $\bar{\nu}_{\tau}$  is not shown because antineutrino- and neutrino-nucleon cross sections become indistinguishable for  $E_{\nu} > 10^6$  GeV: indeed, at very high-energy, i.e low  $x$ , the interaction with *sea* quarks starts to be dominant. Figure 4 shows the distribution of the inelasticity parameter  $y_{CC} = 1 - E_{\tau}/E_{\nu}$ , for different neutrino energies. An average inelasticity  $\langle y \rangle$  can be defined by integrating the distributions given in Figure 4. Few relevant values of  $\langle y \rangle$  are summarized in Table 1 for CC ( $\langle y_{CC} \rangle$ ) and for NC ( $\langle y_{NC} \rangle$ ) interaction.

Figure 5 shows a comparison between a CTEQ4-based parametrization of CC cross section and the corresponding calculation performed with CTEQ6. A substantial agreement is found up to  $10^9$  GeV. We report a maximal discrepancy of about 30% (CTEQ4 higher) at  $10^{12}$  GeV, where the uncertainty due to the lack of knowledge of parton density functions is expected to be overwhelming.

## 4 $\tau$ energy losses

Tau leptons with energy higher than  $10^{16}$  eV may lose a consistent fraction of energy before decaying [45]. A precise knowledge of  $\tau$  energy loss is therefore required in order to draw reliable predictions of expected signal rate at detectors. High-energy  $\tau$ 's propagating through matter mainly interact by quasi-continuous (ionization) and discrete energy loss mechanisms, mainly by photonuclear interaction, direct electron-positron pair production and Bremsstrahlung. Ionization dominates at energy lower than a few TeV while radiative processes become relevant at higher energies.

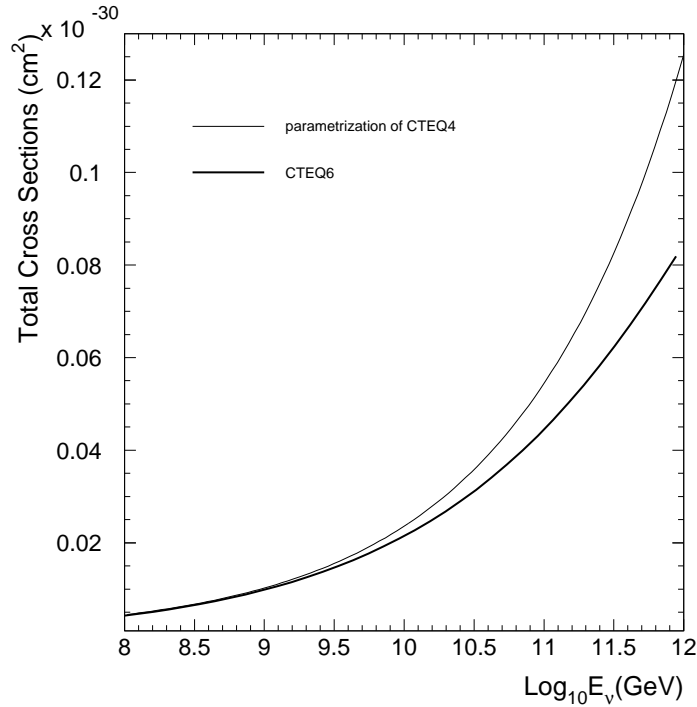


Figure 5: Comparison between a CTEQ4-based parametrization [40] and the CTEQ6 full calculation adopted here. Plots are shown for CC interaction.

The direct electron pair production differential cross section has been firstly calculated by Kelner and Kotov in the framework of QED theory [46]. We have used the well-known parametrization performed by Kokoulin and Petrukhin [47] which considers the corrections for atomic and nuclear form factors.

Bremsstrahlung differential cross section is calculated with the formula derived by Andreev and Bugaev [48], which takes into account the structure of nuclear target (elastic

and inelastic form factors) and the exact contributions due to atomic electrons (screening effect and Bremsstrahlung on electrons).

The complete formulas used here for computing electron pair production and Bremsstrahlung cross sections are the ones reported in Ref. [49], with the only substitution of the muon mass with the  $\tau$  mass. Almost identical formulas are given in Ref. [50] and in Ref. [45], where a slightly simplified formula for Bremsstrahlung (in agreement within a few percent with the one of Ref. [49]) is actually used. A complete list of  $\tau$  matter cross sections written within the same theoretical framework adopted here is also given in Ref. [51].

The photonuclear differential cross section is calculated following the theoretical approach given in Ref. [30]. In that formalism, cross section for photonuclear interaction consists of two terms. The first term, calculated within the Vector Meson Dominance Model, describes the non-perturbative contribution to the electromagnetic structure functions. The parametrization given in Ref. [30] differs from the corresponding well known result of Ref. [52] by a few new terms, negligible for muons but sensible for  $\tau$ 's. The second term, calculated within the framework of the model by Forshaw, Kerley and Shaw (with parameters derived from the last accelerator data), describes the perturbative QCD contribution, not negligible at extremely high energies ( $E_\tau > 10^{15}$  eV). Parametrizations of this term are provided up to  $10^9$  GeV in Ref. [53]. Values at higher energy are obtained by extrapolation. For the calculation of the non-perturbative term, we also considered the recent accelerator data coming from the experiments ZEUS and H1 [54, 55].

The average energy loss for a given discrete process  $k$  can be expressed in terms of the differential cross section,  $d\sigma^k/dv$ , as follows:

$$-\left\langle \frac{dE}{dx} \right\rangle_k = \frac{N_A}{A} E_\tau \int_{v_{min}}^{v_{max}} v \frac{d\sigma^k}{dv}(v, E_\tau) dv = \beta_k(E_\tau) E_\tau \quad , \quad (4.6)$$

where  $N_A$  is the Avogadro's number,  $A$  is the mass number,  $v$  is the fraction of initial energy  $E_\tau$  lost by the  $\tau$  at the occurrence of the process  $k$  and  $x$  is the thickness of the crossed matter, expressed in g/cm<sup>2</sup>.

Figure 6 shows the  $\beta$  values for photonuclear interaction (the most relevant process at high energies), electron pair production and Bremsstrahlung versus the  $\tau$  energy. Figure 7

shows the energy loss due to individual electromagnetic processes and the total average energy loss defined as

$$-\left\langle \frac{dE}{dx} \right\rangle_{tot} = -\left\langle \frac{dE}{dx} \right\rangle_{ionization} + \sum_k \beta_k E_\tau . \quad (4.7)$$

Finally, Figure 8 shows the range of the average energy loss,

$$\mathcal{R}(E_\tau, E_\tau^{min}) = \int_{E_\tau^{min}}^{E_\tau} \frac{dE'_\tau}{-\left\langle dE/dx \right\rangle_{tot}(E'_\tau)} , \quad (4.8)$$

as a function of the initial,  $E_\tau$ , and the final,  $E_\tau^{min}$ ,  $\tau$ -energy. All results shown in Figures 6 - 8 are calculated for standard rock ( $Z=11$ ,  $A=22$ ,  $\rho_s = 2.65 \text{ g/cm}^3$ ). A detailed evaluation of the average (effective) range would require a full stochastic treatment of discrete interactions in order to correctly handle fluctuations. As shown in Ref. [56] and [45], fluctuations may strongly decrease the average range compared to the range of the average energy loss. Results of a full simulation of  $\tau$  propagation through matter are also shown in Ref. [53] and [57].

## 5 The Earth-skimming events

Let us consider an isotropic  $\nu_\tau + \bar{\nu}_\tau$  flux of neutrinos, denoted by  $\Phi_\nu$ , by following the formalism developed in Ref. [27]: the differential flux of charged leptons exiting Earth with energy  $E_\tau$  for unit values of area and time is

$$\frac{d\Phi_\tau(E_\tau, \theta, \phi)}{dE_\tau d\Omega} = \int dE_\nu \frac{d\Phi_\nu(E_\nu, \theta, \phi)}{dE_\nu d\Omega} K(E_\nu, \theta; E_\tau) , \quad (5.9)$$

where  $K(E_\nu, \theta; E_\tau)$  is the probability that a neutrino entering Earth with energy  $E_\nu$  and nadir angle  $\theta$  produces a lepton which exits Earth with energy  $E_\tau$  (see Figure 9). Note that in Eq.(5.9) we have implicitly assumed that in the process  $\nu_\tau + N \rightarrow \tau + X$ , due to the very high energy of  $\nu_\tau$ , the charged lepton is produced along the same direction.

Such a weak event can occur if and only if the following conditions are fulfilled:

- a) the  $\nu_\tau$  with energy  $E_\nu$  has to survive for a distance  $z$  in the Earth;
- b) the neutrino converts into a  $\tau$  in the interval  $z, z + dz$ ;
- c) the created lepton exits Earth before decaying;
- d) the final  $\tau$  energy is  $E_\tau$ .

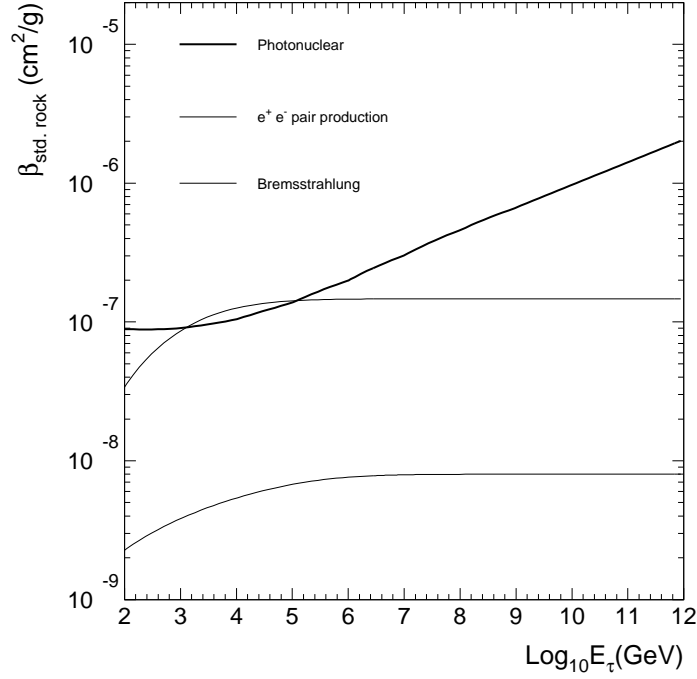


Figure 6:  $\beta$  value for photonuclear interaction (the most relevant process for  $\tau$ 's at high energies), electron pair production and Bremsstrahlung. Results are shown for standard rock ( $Z=11$ ,  $A=22$ ,  $\rho_s = 2.65 \text{ g/cm}^3$ ).

a) The survival probability  $P_a$  for a neutrino with energy  $E_\nu$  crossing the Earth till a certain distance  $z$  is

$$P_a = \exp \left\{ - \int_0^z \frac{dz'}{\lambda_{CC}^\nu(E_\nu, \theta, z')} \right\} , \quad (5.10)$$

where

$$\lambda_{CC}^\nu(E_\nu, \theta, z) = \frac{1}{\sigma_{CC}^{\nu N}(E_\nu) \rho[r(\theta, z)] N_A} \quad (5.11)$$

is the CC interaction length in the rock,  $\rho[r(\theta, z)]$  is the Earth's density at distance  $r$  from its center and  $N_A$  is the Avogadro's number. The distance  $r$  is given by  $r^2(\theta, z) = R_\oplus^2 + z^2 - 2R_\oplus z \cos \theta$ , where  $R_\oplus \simeq 6370 \text{ km}$  is the average Earth radius. Note that, since the CC interaction length in air is almost three order of magnitude larger than in rock, the expression of  $P_a$  does not take into account the atmosphere crossed by the  $\nu_\tau$  before entering the Earth surface.

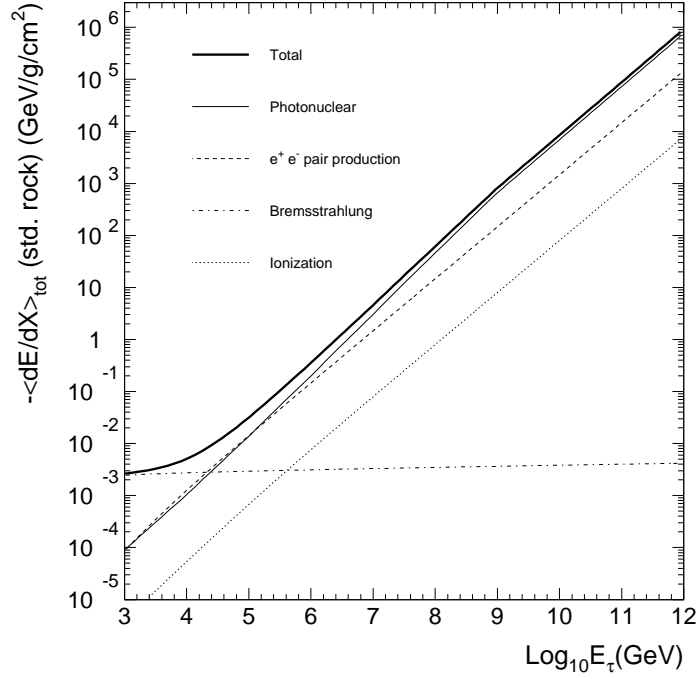


Figure 7: Total average energy loss in standard rock (thick line). Contributions of individual electromagnetic process are also plotted (thin lines). Results are shown for standard rock ( $Z=11$ ,  $A=22$ ,  $\rho_s = 2.65 \text{ g/cm}^3$ ).

b) The probability for  $\nu_\tau \rightarrow \tau$  conversion in the interval  $[z, z + dz]$  is

$$P_b = \frac{dz}{\lambda_{CC}^\nu(E_\nu, \theta; z)} . \quad (5.12)$$

Here a comment is in turn. In order to have an exiting  $\tau$  with enough energy to produce an electromagnetic shower detectable by the FD, the charged lepton cannot travel too much in the rock. On the other side, as already stated before, an EeV neutrino has a  $\lambda_{CC}^\nu \approx 500 \text{ km}$ : thus only quite horizontal  $\nu_\tau$  will be able to produce detectable events and the weak conversion will take place near Earth's surface where the average density is almost constant and equal to  $\rho_s \simeq 2.65 \text{ g/cm}^3$ .

c) The survival probability  $P_c$  for a charged lepton losing energy as it travels through Earth is described by the coupled differential equations:

$$\frac{dP_c}{dz} = -\frac{m_\tau}{c \tau_\tau E_\tau} P_c , \quad (5.13)$$

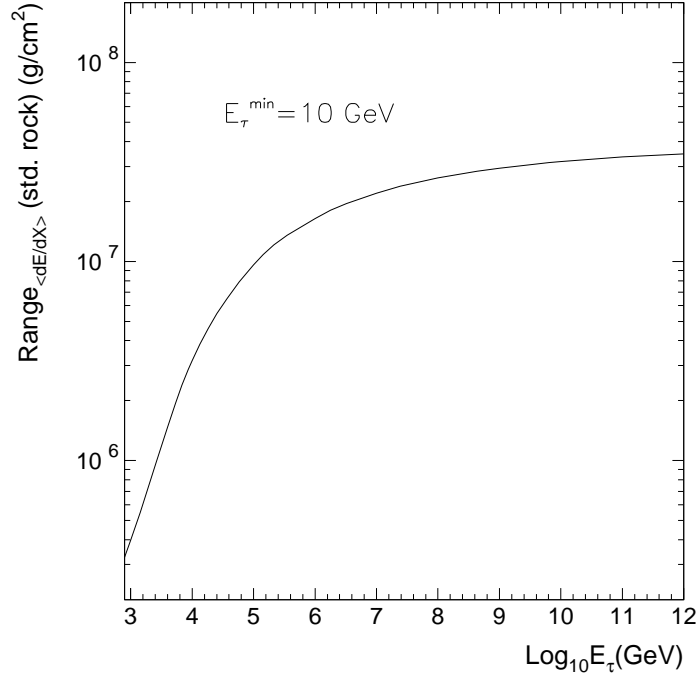


Figure 8: Range of average energy loss as a function of energy  $E_\tau$ .  $E_\tau^{\min}$  has been fixed at 10 GeV. Results are shown for standard rock ( $Z=11$ ,  $A=22$ ,  $\rho_s = 2.65 \text{ g/cm}^3$ ).

$$\frac{dE_\tau}{dz} = -(\beta_\tau E_\tau + \gamma_\tau E_\tau^2) \rho_s . \quad (5.14)$$

Here  $m_\tau = 1.8 \cdot 10^9 \text{ eV}$ ,  $\tau_\tau \simeq 3.4 \cdot 10^{-13} \text{ s}$  denotes the  $\tau$  mean lifetime, whereas the parameters  $\beta_\tau \simeq 0.71 \cdot 10^{-6} \text{ cm}^2 \text{ g}^{-1}$  and  $\gamma_\tau \simeq 0.35 \cdot 10^{-18} \text{ cm}^2 \text{ g}^{-1} \text{ GeV}^{-1}$ , as discussed in Section 4, fairly describe the  $\tau$  energy loss in matter. The previous set of equations can be solved by observing that, following the results presented in section 3 and shown in Table 1, the tau lepton produced at  $z$  carries an average energy which is a function of  $E_\nu$ . Let us denote with  $E_\tau^0 = E_\tau^0(E_\nu) = (1 - \langle y_{CC} \rangle) E_\nu$  such a transferred energy; hence the solution of Eq.s (5.13), (5.14) at the exit point on the Earth surface reads:

$$P_c = (F(E_\nu, E_\tau))^\omega \exp \left\{ -\frac{m_\tau}{c\tau_\tau \beta_\tau \rho_s} \left( \frac{1}{E_\tau} - \frac{1}{E_\tau^0(E_\nu)} \right) \right\} , \quad (5.15)$$

$$E_\tau = \frac{\beta_\tau E_\tau^0(E_\nu) \exp \{ -\rho_s \beta_\tau (2R_\oplus \cos \theta - z) \}}{\beta_\tau + \gamma_\tau E_\tau^0(E_\nu) (1 - \exp \{ -\rho_s \beta_\tau (2R_\oplus \cos \theta - z) \})} , \quad (5.16)$$

where

$$F(E_\nu, E_\tau) \equiv \frac{E_\tau^0(E_\nu)(\beta_\tau + \gamma_\tau E_\tau)}{E_\tau(\beta_\tau + \gamma_\tau E_\tau^0(E_\nu))} , \quad \omega \equiv \frac{m_\tau \gamma_\tau}{c\tau_\tau \beta_\tau^2 \rho_s} . \quad (5.17)$$

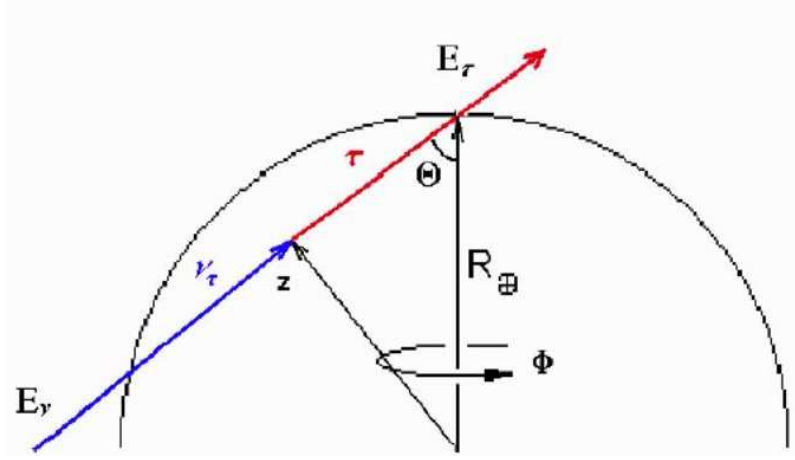


Figure 9: A neutrino  $\nu_\tau$  enters Earth with energy  $E_\nu$  at nadir angle  $\theta$  and azimuthal angle  $\phi$ . It then travels for distance  $z$  before converting to a charged lepton  $\tau$ , which exits Earth with energy  $E_\tau$  [27].

Note that in all previous expressions we have taken into account the vanishing value of  $\alpha_\tau$ . The above results improve the ones obtained in Ref. [27], where a simpler parametrization for the  $\tau$  energy loss was adopted.

d) The energy  $E_\tau$  of the exiting lepton must be consistent with Eq.(5.16). This condition is enforced by the  $\delta$ -function:

$$P_d = \delta \left( E_\tau - \frac{\beta_\tau E_\tau^0(E_\nu) \exp \{-\varrho_s \beta_\tau (2R_\oplus \cos \theta - z)\}}{\beta_\tau + \gamma_\tau E_\tau^0(E_\nu) (1 - \exp \{-\varrho_s \beta_\tau (2R_\oplus \cos \theta - z)\})} \right) . \quad (5.18)$$

By using the expressions for the different probabilities (5.10), (5.12), (5.15), (5.18) the kernel reads

$$K(E_\nu, \theta; E_\tau) = \int_0^{2R_\oplus \cos \theta} P_a P_b P_c P_d dz . \quad (5.19)$$

Once the integration over  $z$  is performed, one gets the simple result

$$K(E_\nu, \theta; E_\tau) = \frac{\sigma_{CC}^{\nu N}(E_\nu) N_A}{E_\tau (\beta_\tau + \gamma_\tau E_\tau)} (F(E_\nu, E_\tau))^\xi \times \exp \left\{ -\frac{m_\tau}{c\tau_\tau \beta_\tau \varrho_s} \left( \frac{1}{E_\tau} - \frac{1}{E_\tau^0(E_\nu)} \right) - 2R_\oplus \cos \theta \sigma_{CC}^{\nu N}(E_\nu) \varrho_s N_A \right\} , \quad (5.20)$$

where

$$\xi \equiv \left( \omega + \frac{\sigma_{CC}^{\nu N}(E_\nu) N_A}{\beta_\tau} \right) . \quad (5.21)$$



Note that Eq.(5.18) also requires to satisfy two conditions. The first one is  $E_\tau^0(E_\nu) \geq E_\tau$  (obviously verified), while the second is

$$\cos \theta \geq \cos \theta_{min} = \frac{1}{2 R_\oplus \beta_\tau \varrho_s} \log (F(E_\nu, E_\tau)) \quad . \quad (5.22)$$

The expression (5.20) for the kernel  $K(E_\nu, \theta; E_\tau)$  allows to compute, for unit of time, the total number of upgoing  $\tau$ 's showering on the Auger apparatus, and thus *potentially* detectable by the FD, which results in

$$\begin{aligned} \frac{dN_\tau}{dt} &= 2\pi S D \int_{E_\nu^{min}}^{E_\nu^{max}} dE_\nu \int_{E_\tau^{th}}^{E_\tau^0(E_\nu)} dE_\tau \int_{\cos \theta_{min}}^1 \frac{d\Phi_\nu(E_\nu)}{dE_\nu d\Omega} \\ &\times K(E_\nu, \theta; E_\tau) \left( 1 - \exp \left\{ -\frac{H m_\tau}{c\tau_\tau E_\tau} \right\} \right) \varepsilon \cos \theta d(\cos \theta) \quad , \quad (5.23) \end{aligned}$$

where we have used the isotropy of the neutrino flux. In Eq.(5.23) the quantity  $S = 3000 \text{ km}^2$  is the geometrical area covered by the Auger apparatus,  $D \sim 10\%$  is the duty cycle for fluorescence detection,  $E_\tau^{th} \simeq 10^{18} \text{ eV}$  is the energy threshold for the fluorescence process, and  $E_\nu^{min}$  is the minimum neutrino energy able to produce a  $\tau$  at threshold. The upper bound on neutrino energy,  $E_\nu^{max}$ , is a property of the neutrino flux. The exponential term in the r.h.s. of Eq.(5.23) accounts for the decay probability of a  $\tau$  (showering probability) in a distance  $H$  from the exit point. In order to be sure that the  $\tau$  decays on the apparatus one should consider  $H$  as a function of the exit point; here we assume for simplicity an average  $H \simeq 30 \text{ km}$  which however leads to a reliable estimate of the number of events. The trigger efficiency  $\varepsilon$ , as can be seen in Ref. [1], can be taken equal to unity for these value of  $\tau$  energy.

In Eq.(5.23) the integration over  $\cos \theta$  can be easily performed and this yields to

$$\frac{dN_\tau}{dt} = D \int_{E_\nu^{min}}^{E_\nu^{max}} dE_\nu \frac{d\Phi_\nu(E_\nu)}{dE_\nu d\Omega} A(E_\nu) \quad , \quad (5.24)$$

where the *effective aperture* of the apparatus is here defined as

$$\begin{aligned} A(E_\nu) &= \frac{\pi S}{2 R_\oplus^2 N_A \varrho_s^2} \int_{E_\tau^{th}}^{E_\tau^0(E_\nu)} dE_\tau \frac{(F(E_\nu, E_\tau))^\omega}{E_\tau (\beta_\tau + \gamma_\tau E_\tau)} \\ &\times \exp \left\{ -\frac{m_\tau}{c\tau_\tau \beta_\tau \varrho_s} \left( \frac{1}{E_\tau} - \frac{1}{E_\tau^0(E_\nu)} \right) \right\} \left( 1 - \exp \left\{ -\frac{H m_\tau}{c\tau_\tau E_\tau} \right\} \right) \varepsilon \\ &\times \frac{1}{\sigma_{CC}^{\nu N}} \left[ \left( 1 + \frac{\sigma_{CC}^{\nu N} N_A}{\beta_\tau} \log (F(E_\nu, E_\tau)) \right) \right. \\ &\left. - \left( 1 + 2 R_\oplus \sigma_{CC}^{\nu N} \varrho_s N_A \right) \exp \left\{ -2 R_\oplus \sigma_{CC}^{\nu N} \varrho_s N_A \right\} (F(E_\nu, E_\tau))^{\sigma_{CC}^{\nu N} N_A / \beta_\tau} \right]. \quad (5.25) \end{aligned}$$

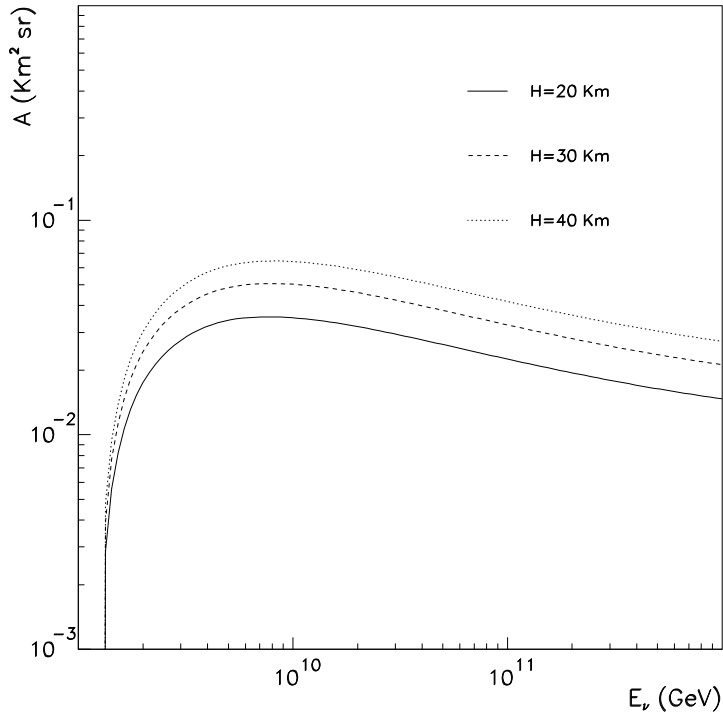


Figure 10: The *effective aperture*,  $A(E_\nu)$ , as defined in Eq.(5.25).

In Figure 10  $A(E_\nu)$  is plotted versus the neutrino energy. This quantity shows a maximum, near  $E_\nu \sim 10^{10}$  eV, of the order of one tenth  $\text{km}^2 \cdot \text{sr}$ , which is, however, sensibly dependent on the parameter  $H$ . Similar results, even though obtained via a Monte Carlo simulation, are reported in Ref. [28].

In Table 2 the number of  $\tau$ -shower Earth-skimming events per year expected at the FD of PAO is reported, calculated according to Eq.s (5.24) and (5.25). The predictions concern the neutrino fluxes reported in Figure 1 and 2, namely the Waxman-Bahcall limit (GZK-WB), the maximum possible flux (GZK-H), the case for 1/5 contribution in the EGRET flux (GZK-L), the neutrino flux from topological defects (TD) and in the model of new hadrons (NH).

$dN_\tau/dt$ at FD	GZK-WB	GZK-L	GZK-H	TD	NH
# of events/year	0.02	0.04	0.09	0.11	0.25

Table 2: Number of events per year at the FD of PAO for the different neutrino models reported in Figures 1 and 2.

In Figure 11 the energy spectra of the  $\tau$ -shower Earth-skimming events per year at

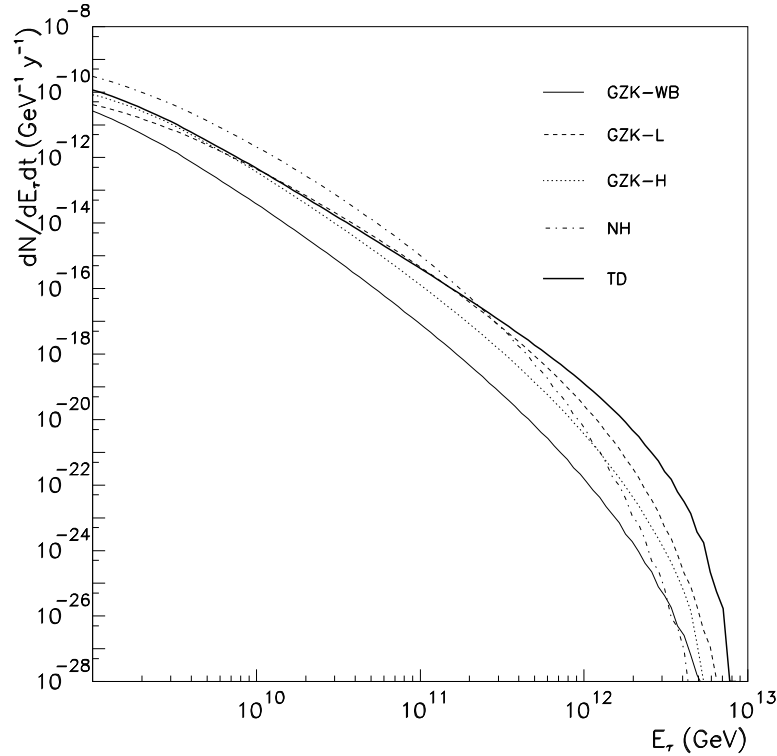


Figure 11: The quantity  $dN_\tau/dE_\tau dt$  is plotted for the different neutrino models reported in Figures 1 and 2.

the FD are plotted for the different neutrino models reported in Figures 1 and 2. As expected, the maximum number of events is obtained near the FD threshold of  $\simeq 1$  EeV, even though the maxima of neutrino fluxes are at higher energy. This can be easily understood by observing that tau leptons emerging inside the Auger surface with large energy and almost horizontally will probably decay far from the apparatus and are thus undetectable by the FD. By using the integrand in the r.h.s. of Eq.(5.24) it is possible to determine the typical angle,  $\alpha_{max} = \theta_{max} - \pi/2$ , with respect to the horizontal of the Earth-skimming events, where  $\theta_{max}$  denotes the nadir angle for which the kernel of Eq.(5.24) has the maximum. This quantity, which is a function of  $\sigma_{CC}^{\nu N}$  and thus of the neutrino energy, is plotted in Figure 12.

As pointed out for example in Ref. [25],  $\nu_\tau$  crossing deeply the Earth could experience a regeneration *phenomenon*, as shown for example in Figure 13 for a second order process, which would eventually allow their propagation till the experimental apparatus. Furthermore, this process would also be characterized by the possible production of sec-

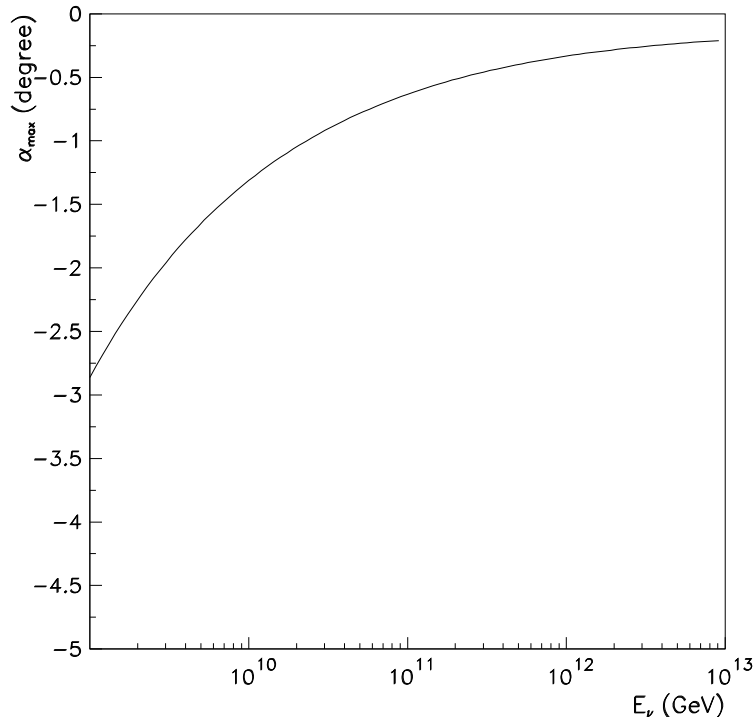


Figure 12: The most likely exit angle with respect to the horizontal for the exiting  $\tau$  is plotted versus the energy of the primary neutrino.

ondary neutrinos at the CC vertex which means additional contributions to the number of events for the detector. Unfortunately, due to the large FD threshold, this effect results to be absolutely irrelevant for PAO. Higher order processes, like the one of Figure 13 even including NC interactions, would also give negligible modifications to the numbers presented in Table 2.

## 6 Conclusions

Ultra High Energy  $\nu_\tau$ 's ( $E_\nu \geq 1 EeV$ ) could have real detection chances at giant surface apparatus like PAO. Unfortunately, the value of the neutrino-nucleon cross section at this energy if, on one side, makes the atmosphere essentially transparent to crossing  $\nu$ 's, on the other side makes the Earth essentially opaque for these energetic particles. Nevertheless, a very narrow detection window is still opened. It is restricted to the almost horizontal tau neutrinos which, crossing distance in the Earth of the order of their interaction length, might produce  $\tau$ -shower Earth-skimming events potentially detectable by the Auger FD.

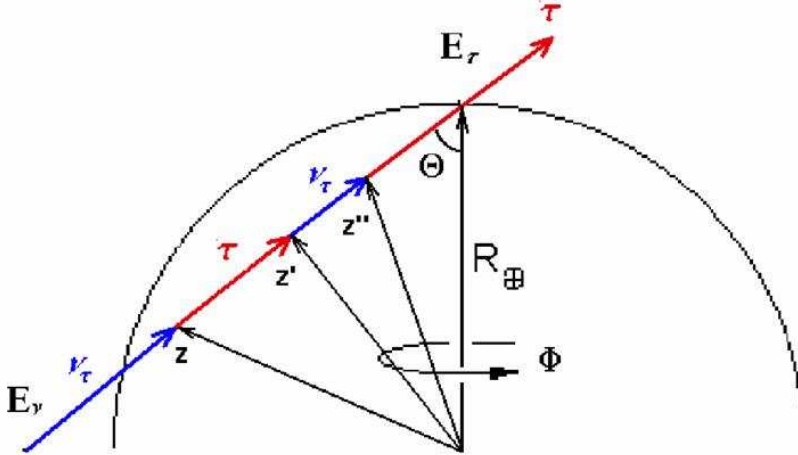


Figure 13: Second order regeneration process for  $\nu_\tau$ .

In the present analysis, for a representative sample of  $\nu_\tau$  fluxes either produced as *cosmogenic neutrinos* or in more exotic scenarios, the number of  $\tau$ -shower Earth-skimming events per year expected at the FD of the Pierre Auger Observatory has been computed. Since this quantity is critically dependent on the neutrino-nucleon cross section, we have updated its calculation by using the CTEQ6 [29] parton density functions in the DIS factorization scheme. The evaluation based on CTEQ6 results to be sensibly different, at least at high energy, from the analogous quantity obtained from the previous parton density functions of CTEQ4 (see Figure 5). A decrease of  $\sigma_{CC}^{\nu N}$ , since it enlarges the neutrino interaction length, allows the emerging of tau leptons with a smaller nadir angle (less horizontal) and thus increases the number of Earth-skimming events. In the relevant region of  $E_\nu$ , we essentially have  $dN_\tau/dt \propto (\sigma_{CC}^{\nu N})^{-1}$ ; thus a factor 1/2 in the neutrino-nucleon cross section leads to an almost double number of events at FD. Nevertheless, the variation shown in Figure 5 points out once more the level of theoretical uncertainty still present on  $\sigma_{CC}^{\nu N}$  and essentially due to the poor experimental knowledge of parton density functions for very small  $x$ .

Our results for the number of events per year at the FD of the Pierre Auger Observatory for the different neutrino models reported in Figure 1 and Figure 2 are presented in

Table 2. For a five years detection campaign of PAO (South plus North) we essentially have to multiply these numbers by a factor ten and thus at least the exotic models could produce detectable events. However, it is worth noticing that this estimate has been performed by assuming a rather conservative point of view concerning the possibility of showering on the apparatus for the emerging  $\tau$ 's. We have used an average value for the parameter  $H$  which essentially allows only one particle over three to decay inside the apparatus. In a paper in progress a more sophisticated simulation is being performed by taking into account the real morphology of PAO site, thus studying on an event by event basis the possible  $\tau$  tracks. This analysis should slightly increase the numbers presented in Table 2 which however represents a significant estimate of the number of events at FD. It is worth stressing once more that these results strongly depend on the extrapolation of the neutrino cross section to high energies, and thus could be affected by possible new physics on scales above TeV.

It is worth noticing that our results cannot be straightforwardly compared with the similar ones contained in Ref. [28] where a Monte Carlo simulation has been performed, using different cross section and fluxes and considering the Surface Detector, corresponding to a duty cycle of order unity. Nevertheless, their numerical results, seem to be not far from our estimate (see Figure 10), at least concerning the total aperture of the apparatus, even though our analysis is, however, restricted to the FD only.

## Acknowledgments

We would like to thank I. A. Sokalski and E. Bugaev for the extremely helpful suggestions on the matter of  $\tau$  photonuclear interaction. The authors would also like to thank M. Ambrosio, F. Guarino and S. Pastor for valuable comments. Work of D.S. supported in part by NASA ATP grant NAG5-13399.

## References

- [1] Auger Collaboration, *The Pierre Auger Project Design Report*, FERMILAB-PUB-96-024.

- [2] P. Niessen [the AMANDA Collaboration], astro-ph/0306209.
- [3] C. Spiering *et al.* [The BAIKAL Collaboration], astro-ph/0404096.
- [4] F. Halzen, Am. Astron. Soc. Meeting 192, #62 28 (1998).
- [5] I. Kravchenko, astro-ph/0306408.
- [6] T. Montaruli *et al.* [ANTARES Collaboration], physics/0306057.
- [7] For general information see <http://www.nestor.org.gr> .
- [8] P. Gorham et al. (ANITA collaboration), <http://www.ps.uci.edu/~barwick/anitaprop.pdf>.
- [9] For general information see <http://www.euso-mission.org>.
- [10] J. Linsley, Phys. Rev. Lett. **10** (1963) 146; Proc. 8th ICRC **4** (1963) 295.
- [11] See e.g. M.A. Lawrence, R.J. Reid and A.A. Watson, J. Phys. G **17** (1991) 733, and references therein.
- [12] D.J. Bird et al., Phys. Rev. Lett. **71** (1993) 3401; Astrophys. J. **424** (1994) 491; *ibid.* **441** (1995) 144.
- [13] N.N. Efimov et al., Proc. International Symposium on *Astrophysical Aspects of the Most Energetic Cosmic Rays*, eds. M. Nagano and F. Takahara (World Scientific Singapore, 1991) p.20; B.N. Afanasiev, Proc. of the International Symposium on *Extremely High Energy Cosmic Rays: Astrophysics and Future Observatories*, ed. M. Nagano (Institute for Cosmic Ray Research, Tokyo, 1996), p.32.
- [14] M. Takeda et al., Phys. Rev. Lett. **81** (1998) 1163; N. Hayashida et al., Astrophys. J. **522** (1999) 225. For general information see <http://www-akeno.icrr.u-tokyo.ac.jp/AGASA/>.
- [15] D. Kieda et al., Proc. of the 26th ICRC, Salt Lake, 1999; T. Abu-Zayyad et al., HiRes Collaboration, astro-ph/0208243. For general information see <http://www.physics.utah.edu/Resrch.html>.

- [16] V. S. Beresinsky and G. T. Zatsepin, Phys. Lett. B **28**, 423 (1969); V. S. Berezinsky and G. T. Zatsepin, Sov. J. Nucl. Phys. 11 (1970) 111 [Yad. Fiz. 11 (1970) 200].
- [17] P. Sreekumar *et al.*, Astrophys. J. **494**, 523 (1998).
- [18] O. E. Kalashev, V. A. Kuzmin, D. V. Semikoz and G. Sigl, Phys. Rev. D **66**, 063004 (2002).
- [19] D. V. Semikoz and G. Sigl, JCAP **0404**, 003 (2004).
- [20] D. Fargion, astro-ph/9704205.
- [21] F. Halzen and D. Saltzberg, Phys. Rev. Lett. **81**, 4305 (1998).
- [22] F. Becattini and S. Bottai, Astropart. Phys. **15**, 323 (2001).
- [23] S. I. Dutta, M. H. Reno, I. Sarcevic and D. Seckel, Phys. Rev. D **63**, 094020 (2001).
- [24] S. I. Dutta, M. H. Reno and I. Sarcevic, Phys. Rev. D **66**, 077302 (2002).
- [25] J. F. Beacom, P. Crotty and E. W. Kolb, Phys. Rev. D **66**, 021302 (2002).
- [26] A. Kusenko and T. J. Weiler, Phys. Rev. Lett. **88**, 161101 (2002).
- [27] J. L. Feng, P. Fisher, F. Wilczek and T. M. Yu, Phys. Rev. Lett. **88**, 161102 (2002).
- [28] X. Bertou, P. Billoir, O. Deligny, C. Lachaud and A. Letessier-Selvon, Astropart. Phys. **17**, 183 (2002).
- [29] <http://user.pa.msu.edu/wkt/cteq/cteq6/cteq6pdf.html>. See also: J. Pumplin *et al.* *hep-ph/0201195*, D. Stump *et al.* *hep-ph/0303013*.
- [30] E. V. Bugaev, Yu. V. Shlepin, Phys. Rev. D **67**, 034027 (2003). See also *hep-ph/0203096 v5*.
- [31] P. Sreekumar *et al.*, Astrophys. J. **494**, 523 (1998) [*astro-ph/9709257*]; A. W. Strong, I. V. Moskalenko and O. Reimer, *astro-ph/0306345*; *astro-ph/0405441*.
- [32] V. S. Berezinsky and A. Yu. Smirnov, Ap. Sp. Sci. **32**, 461 (1975).



- [33] E. Waxman and J. N. Bahcall, Phys. Rev. D **59**, 023002 (1999) [hep-ph/9807282].
- [34] O. E. Kalashev, V. A. Kuzmin and D. V. Semikoz, astro-ph/9911035; Mod. Phys. Lett. A **16**, 2505 (2001) [astro-ph/0006349].
- [35] M. Kachelriess, D. V. Semikoz and M. A. Tortola, Phys. Rev. D **68**, 043005 (2003) [hep-ph/0302161].
- [36] P. Bhattacharjee and G. Sigl, Phys. Rept. **327**, 109 (2000) [astro-ph/9811011].
- [37] N. G. Lehtinen, P. W. Gorham, A. R. Jacobson and R. A. Roussel-Dupre, Phys. Rev. D **69**, 013008 (2004) [astro-ph/0309656].
- [38] P. W. Gorham, C. L. Hebert, K. M. Liewer, C. J. Naudet, D. Saltzberg and D. Williams, astro-ph/0310232.
- [39] S. Hannestad, JCAP **0305**, 004 (2003) [arXiv:astro-ph/0303076].
- [40] R. Gandhi, C. Quigg, M. Reno, I. Sarcevic, Phys. Rev. D **58**, 093009 (1998).
- [41] V. N. Gribov and L. N. Lipatov, Yad. Fiz. **15**, 1218 (1972) [Sov. J. Nucl. Phys. **15**, 675 (1972)].
- [42] L. N. Lipatov, Sov. J. Nucl. Phys. **20**, 94 (1975) [Yad. Fiz. **20**, 181 (1974)].
- [43] Y. L. Dokshitzer, “Calculation Of The Structure Functions For Deep Inelastic Scattering And E+ Sov. Phys. JETP **46**, 641 (1977) [Zh. Eksp. Teor. Fiz. **73**, 1216 (1977)].
- [44] G. Altarelli and G. Parisi, Nucl. Phys. B **126**, 298 (1977).
- [45] S. I. Dutta, M. H. Reno, I. Sarcevic, Phys. Rev. D **63**, 094020 (2001).
- [46] S. R. Kelner, V. V. Kotov, Sov. J. Nucl. Phys. **7**, 237 (1968).
- [47] R. P. Kokoulin, A. A. Petrukhin, Proc. of 12<sup>th</sup> Int. Cosmic Ray Conf. (ICRC 71), Hobart **6**, A2436 (1971).
- [48] Yu. M. Andreev, E. V. Bugaev, Phys. Rev. D **55**, 1233 (1997).

- [49] S. Bottai, L. Perrone, Nucl. Instr. and. Meth. A **459**, 319 (2001).
- [50] W. Lohmann, R. Kopp, R. Voss, CERN yellow report 85-03 (1985).
- [51] I. A. Sokalski, E. V. Bugaev, S. I. Klimushin, Phys. Rev. D **64**, 074015 (2001).
- [52] L. B. Bezrukov, E. V. Bugaev, Sov. J. Nucl. Phys. **33**, 635 (1981).
- [53] E. Bugaev, T. Montaruli, Y. Shlepin, I. Sokalski, hep-ph/0312295 v2.
- [54] M. Derrick et al., ZEUS Collaboration, Phys. Lett. B **293**, 465 (1992).
- [55] T. Ahmed et al., H1 Collaboration, Phys. Lett. B **299**, 374 (1993).
- [56] P. Lipari and T. Stanev, Phys. Rev. D **44**, 3543 (1991).
- [57] S. Bottai and S. Giurgola, Astropart. Phys. **18**, 539 (2003).